Journal for Technology and Science
Homepage : https://journal.antispublisher.com/index.php/IPTEKS
Email : admin@antispublisher.com

e-ISSN : 3047-4337
JOTECH, Vol. 3, No. 4, October 2026
Page 379-389
© 2026 JOTECH :
Journal for Technology and Science

Eradication Efficiency of Selenium and Silver Nanoparticles Against Staphylococcus Bacteria

Khawla S. Mohammed
Tikrit University, Iraq

Check for updates
OPEN ACCESS

DOI : https://doi.org/10.61796/ipteks.v3i4.648

Sections Info

Article history:
Submitted: July 07, 2026
Final Revised: August 16, 2026
Accepted: September 04, 2026
Published: October 25, 2026

Keywords:
Silver nanoparticles
Selenium nanoparticles
Antibacterial activity
Minimum inhibitory concentration
Minimum bactericidal concentration
Nanoparticle characterization
Salmonella

ABSTRACT

Objective: *This study evaluates the antibacterial efficacy of chemically synthesized silver nanoparticles (AgNPs) and selenium nanoparticles (SeNPs) and characterizes their physicochemical properties.* ***Method:*** *AgNPs were synthesized by citrate-mediated reduction of silver nitrate, whereas SeNPs were prepared by reducing sodium selenite with ascorbic acid in the presence of polysorbate. The nanoparticles were characterized by UV-Visible spectroscopy, scanning electron microscopy (SEM), Fourier-transform infrared spectroscopy (FT-IR), and X-ray diffraction (XRD). Antibacterial activity was assessed using agar well diffusion, minimum inhibitory concentration (MIC), and minimum bactericidal concentration (MBC) assays.* ***Results:*** *AgNPs and SeNPs showed maximum UV-Visible absorbance at 455 nm and 262 nm, respectively. SEM indicated mean particle sizes of 22.44±0.68 nm for AgNPs and 41.34±1.28 nm for SeNPs. Antibacterial inhibition increased with nanoparticle concentration, while AgNPs generally produced stronger inhibition and lower MIC/MBC values than SeNPs. Novelty: The study provides a direct comparative assessment of silver and selenium nanoparticles synthesized and tested under the same experimental framework, linking physicochemical characterization with concentration-dependent antibacterial performance.*

INTRODUCTION

Metallic nanoparticles have attracted substantial interest because nanoscale dimensions can produce high surface-area-to-volume ratios and physicochemical properties that differ from bulk materials [1]. Silver nanoparticles (AgNPs), in particular, have been widely investigated as a new generation of antimicrobial materials [2]. Their synthesis route, particle size, surface chemistry, and colloidal stability can influence biological activity and practical performance [3]. The growing problem of bacterial resistance has increased interest in alternative antimicrobial strategies that can complement conventional agents [4]. Experimental evidence has shown that silver nanoparticles and silver-containing materials can inhibit microbial growth through multiple physicochemical interactions [5]. Nanosilver has consequently been explored for disinfection and other antibacterial applications [6]. Its medical relevance has also been discussed in relation to infection control and wound management [7]. Nanocrystalline silver-containing products have further demonstrated clinical utility in burn management [8]. Beyond antimicrobial use, silver nanoparticles have been investigated as catalysts in multicomponent chemical reactions [9]. Silver-based nanostructures have also been developed for catalytic oxidation applications [10]. Radiolytic and supported synthesis routes illustrate the versatility of AgNP preparation for functional materials [11]. Conductive silver-polyaniline-silica nanocomposites

additionally demonstrate the potential of silver nanomaterials in biosensing [12]. Selenium nanoparticles (SeNPs) are another promising nanomaterial because their synthesis and surface stabilization can generate systems with synergistic antibacterial properties [13]. Based on these considerations, the present study compares chemically synthesized AgNPs and SeNPs through spectroscopic and structural characterization and evaluates their concentration-dependent antibacterial performance using inhibition-zone, MIC, and MBC measurements.

The purpose of determining MICO's minimum inhibitory concentration and the MBC's minimum lethal concentration of the nanomaterials included in the study, a series of graduated dilutions of silver nanoparticles and selenium nanotubes in the test tubes will be prepared using the nutrient broth, namely (0.25-500) Microgram/ml after which the tubes will be smeared by 0.1 ml of 24-hour germ farm and containing approximately 1.6×106 cells /ML, as previously prepared with the preparation of a test tube container on the nutrient broth fertilized with germ represented by control No. (1) and a second test tube containing the nutrient broth only represented by control No. (2) to be returned experiment in the event that the turbidity does not appear in the control tube number (1) or in the case of its appearance in the control tube number (2). Then all the pipes will be incubated at a temperature of °37 m for 48 hours and then removed from the incubator and the value of the minimum inhibitory concentration of the prepared nanomaterial will be determined, which represented the least concentration of the material to prevent the emergence of a clear turbidity For the naked eye in the liquid implant culture, the minimum lethal concentration value of the nanomaterial will be determined by taking 0.1 ml of liquid culture and all pipes that will notshow a clear turbidity and were planted on container implant dishes Nourishing agar and incubating it at °37m for 24 hours determined the minimum lethal concentration value of the nanomaterial, which, like the least concentration of the substance, reduced the number of germ colonies by 99.9% of the original plant.

RESEARCH METHOD

Silver Nanoparticle Synthesis

Silver nanoparticles (AgNPs) were synthesized using a wet chemical reduction method adapted from Fang et al. [14]. A silver nitrate solution was prepared by dissolving 0.0169 g $AgNO_3$ in 100 mL deionized water and stirring at 45°C. A 1% sodium citrate solution was separately prepared by dissolving 1 g sodium citrate in 100 mL distilled water. Twenty milliliters of the $AgNO_3$ solution were heated to 90°C for 5 min, followed by gradual addition of 2.5 mL sodium citrate. The appearance of a pale-yellow color indicated reduction. The mixture was stirred for 15 min, centrifuged at 6000 rpm for 10 min, dried at 100°C for 36 h, and stored until analysis.

Selenium Nanoparticle Synthesis

Selenium nanoparticles (SeNPs) were produced by chemical reduction of sodium selenite using ascorbic acid as the reducing agent and polysorbate as a stabilizer, following the general approach described by Vahdati and Tohidi Moghadam [13]. Thirty grams of sodium selenite were dissolved in 90 mL deionized water. Ten milliliters of 56.7 mmol ascorbic acid were gradually added while the mixture was magnetically stirred at 45°C. During mixing, approximately 10 µL polysorbate was added per 2 mL ascorbic acid. The mixture was maintained for 30 min until the color changed from white to red, after which the SeNPs were collected by centrifugation at 12,000 rpm and stored until use.

Nanoparticle Characterization

UV-Visible spectra of AgNPs and SeNPs were recorded five days after preparation over 200-800 nm after color stabilization. SEM was used to determine particle size and morphology by depositing nanoparticle suspensions on carbon-coated copper supports and allowing them to dry before examination. FT-IR analysis was used to identify functional groups; dried nanoparticle powders were scanned using a Tensor 27 FT-IR spectrophotometer, consistent with infrared characterization approaches for nanoparticles [15]. XRD analysis was performed using a Phillips PW1830 system operated at 40 kV and 20 mA to evaluate crystallinity and structural characteristics. Similar nanomaterial characterization procedures have been reported for metal-oxide nanoparticle systems [16].

Bacterial Suspension Preparation

The bacterial suspension was prepared by streaking the test bacteria on nutrient medium and incubating at 37°C for 24 h. Growth was transferred to a slant nutrient medium and incubated again at 37°C for 24 h. Bacterial growth was washed from the slant with 10 mL nutrient broth, mixed thoroughly, and transferred to a sterile tube. The suspension was standardized spectrophotometrically at 580 nm, with bacteria-free nutrient broth used as the blank.

Antibacterial Activity, MIC, and MBC

Antibacterial activity was evaluated using the agar well diffusion method. Sterile nutrient agar was poured into Petri dishes, inoculated with the prepared bacterial suspension, and wells of 6 mm diameter were formed. Nanoparticle preparations at 25, 50, 100, and 200 mg/mL were added to the wells, while phosphate-buffered saline/deionized water served as the control. Plates were incubated at 37°C for 24 h and inhibition zones were measured in millimeters. MIC and MBC were determined by serial broth dilution. The MIC was defined as the lowest concentration preventing visible turbidity, whereas the MBC was the lowest concentration producing at least a 99.9% reduction in the original bacterial inoculum, consistent with established nanoparticle susceptibility procedures [17]. Agar diffusion, MIC, and MBC measurements were interpreted as complementary indicators of antibacterial potency [18].

RESULTS AND DISCUSSION

Result

Preparation of Nanomaterials

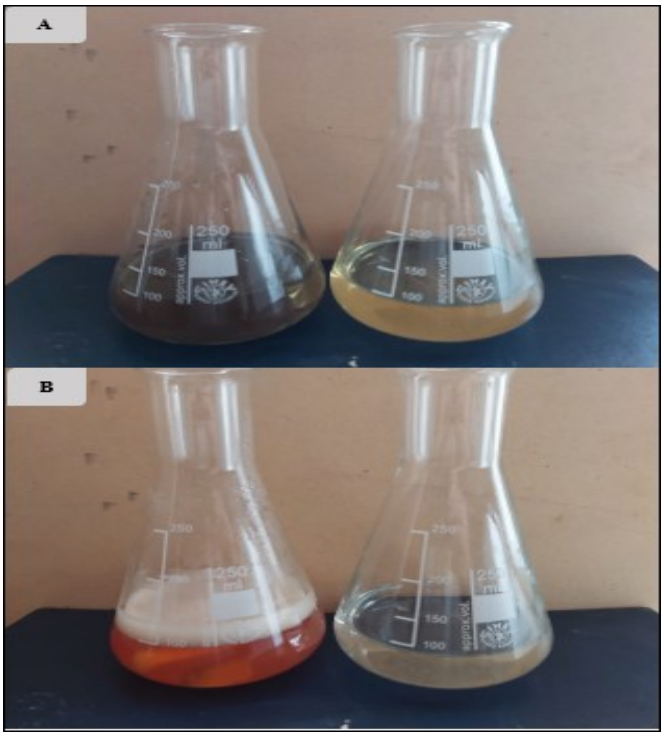


Figure 1. Preparation of nanoparticles (A) Silver nanoparticles (B) Selenium nanoparticles

UV-Visible Spectrum Analysis

The UV-visible spectrum analysis results for the produced silver and selenium nanoparticles, as depicted in Figure (2), demonstrate that the highest absorbance was seen at 455 nm and 262 nm, respectively.

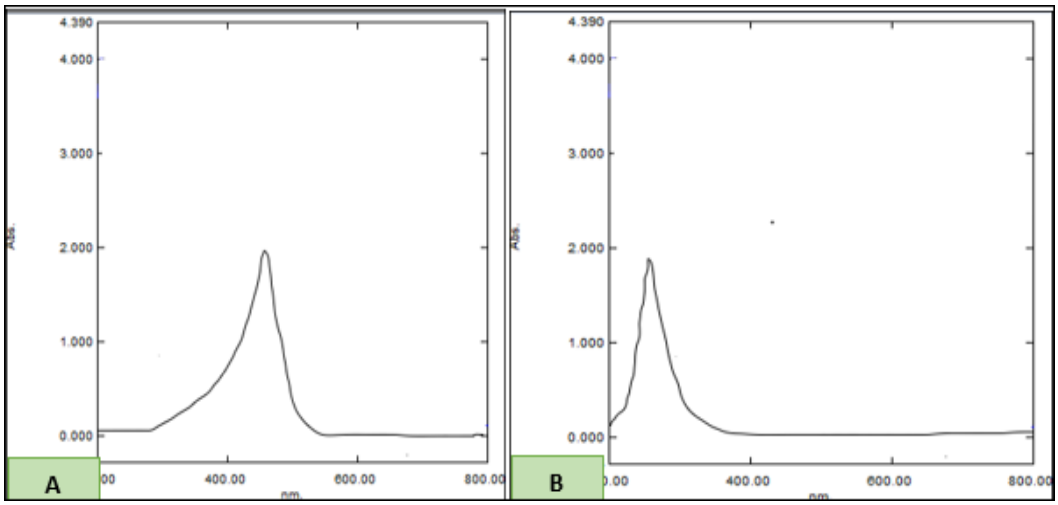


Figure 2. UV-visible spectrum analysis (A) Silver nanoparticles (B) Selenium nanoparticles

Scanning Electron Microscope (SEM) Analysis

SEM examination was conducted on the silver and selenium nanoparticles that were generated in order to ascertain their size and shape. The analysis revealed that the mean size of 100 silver nanoparticles was 22.44±0.68 nm, with a range of 14.52 to 27.66 nm. Additionally, all the nanoparticles exhibited a spherical morphology. The selenium nanoparticles exhibited an average diameter of 41.34±1.28 nm, with a range of 33.45 to 46.1 nm. Their morphology ranged from spherical to oval, as depicted in Figure 3.

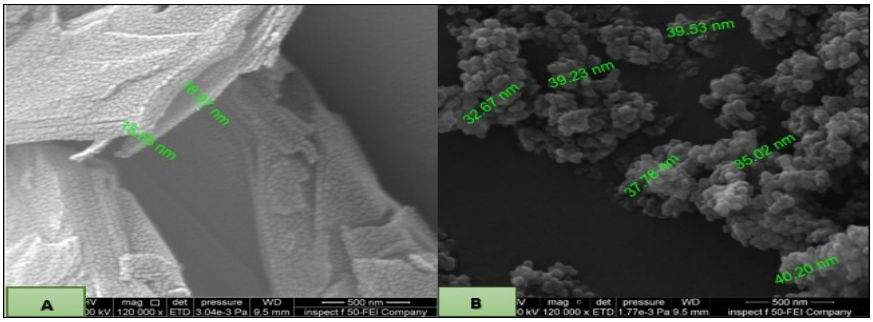


Figure 3. Scanning electron microscope (A) Silver nanoparticles (B) Selenium nanoparticles

Fourier Transform Infrared (FT-IR) Spectrophotometry

The chemically produced silver and selenium nanoparticle samples were analyzed using FT-IR spectrum analysis to detect the functional groups present. Figure (4-A) displays the FT-IR spectra of the produced silver nanoparticles. The analysis reveals the existence of significant diagnostic peaks in the silver nanoparticle sample at specific wavenumbers: 3416.41, 1784.51, 1651.31, 1563.06, 1424.32, 1421.79, 1321.59, 942.53, 679.31, and 588.83 cm−1. The produced selenium nanoparticles are depicted in Figure (4-B) in their FT-IR spectra. The results indicate the existence of significant diagnostic peaks at specific wavenumbers: 3417.86, 2934.09, 2840.79, 1780.5, 1717.65, 1583.91, 1452.75, 1344.7, 1290.73, 1132.57, 1055.42, and 1010.7 cm−1.

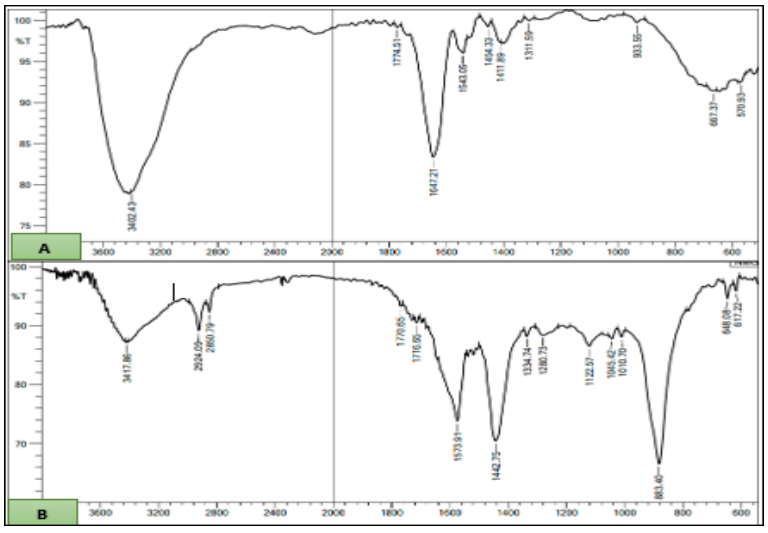


Figure 4. Infrared spectrum (A) Silver nanoparticles (B) Selenium nanoparticles

X-ray Diffraction

The chemically generated silver and selenium nanoparticle samples were analyzed using X-ray diffraction analysis to ascertain their crystalline structure and gain understanding of their particle size. The XRD analysis revealed that the silver nanoparticles generated possess a cubic morphology, and the observed crystalline planes matched to diffraction angles of 38.28, 45.47, 65.64, and 78.62 degrees, as depicted in Figure 5 A. The produced selenium nanoparticle sample exhibited distinct crystalline planes at specific diffraction angles ranging from 19.3 to 74.6 degrees, as observed in Figure 5. B.

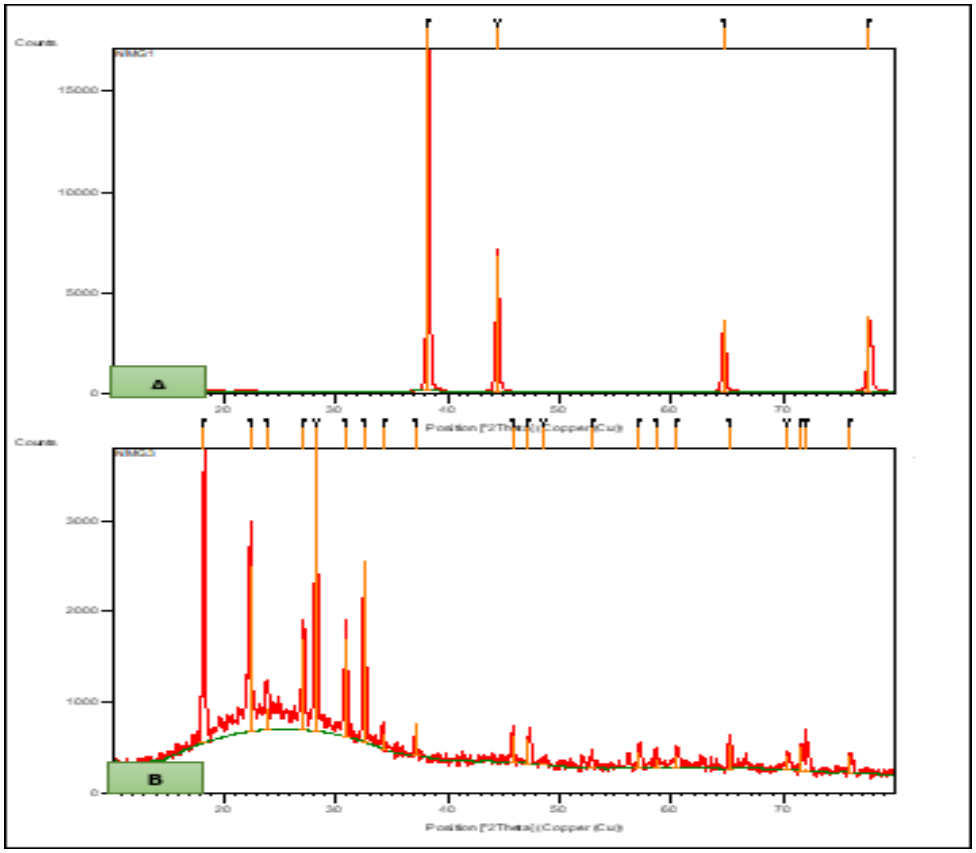


Figure 5. X-ray diffraction (A) Silver nanoparticles (B) Selenium nanoparticles.

Table 1. shows the MIC and MBC values recorded for the silver and selenium nanoparticles tested against eight Salmonella isolates.

Sample no.	Selenium nanoparticles		Silver nanoparticles	
	Minimum letahl concentration)mg\ml(	Minimum inhibitory concentration)mg\ml(	Minimum letahl concentration)mg\ml(	Minimum inhibitory concentration)mg\ml(
Isolate no.1	300	100	100	50

Sample no.	Selenium nanoparticles		Silver nanoparticles	
	Minimum letahl concentration)mg\ml(	Minimum inhibitory concentration)mg\ml(	Minimum letahl concentration)mg\ml(	Minimum inhibitory concentration)mg\ml(
Isolate no.2	320	50	300	90
Isolate no.3	350	90	160	80
Isolate no.4	170	50	180	50
Isolate no.5	180	160	160	40
Isolate no.6	690	360	170	40
Isolate no.7	300	180	90	10
Isolate no.8	360	200	100	80

Silver nanoparticles exhibited minimum inhibitory concentration (MIC) values ranging from 10-80 µg/mL and minimum bactericidal concentration (MBC) values ranging from 90-300 µg/mL. The MIC (Minimum Inhibitory Concentration) values of selenium nanoparticles ranged from 50-360 µg/mL, whereas the MBC (Minimum Bactericidal Concentration) values ranged from 170-690 µg/mL. The silver nanoparticles exhibited superior antibacterial efficacy, necessitating lower doses to impede bacterial proliferation.

Table 2. presents the zones of growth inhibition measured around nanoparticle-loaded wells at each concentration tested on agar diffusion plates.

Selenium nanoparticles	Silver nanoparticles	Concentration used mg\ml
7.53±0.08Da	7.41±0.56Da	25
8.53±0.52Cb	9.03±0.18Ca	50
10.90±0.43Bb	11.82±0.74Ba	100
12.03±0.32Ab	13.73±0.8Aa	200
0±0Ea	0±0Ea	BPS
0.272		**LSD**

The LSD value is the smallest meaningful difference. Therefore, any variations between groups or concentrations more than 0.272 mm would be deemed statistically significant at a significance level of $p<0.05$. The following are the important results presented:

1. The antibacterial activity/growth inhibition against Salmonella increased as the concentration of both silver and selenium nanoparticles increased.
2. The silver nanoparticles exhibited much greater antibacterial efficacy than the selenium nanoparticles at every concentration examined.

The control group exposed to 0 nanoparticles (BPS) did not exhibit any growth inhibition. More precisely: • The concentrations that were tested were 25, 50, 100, and 200 mg/mL. • The size of the zone of inhibition (measured in mm) is used to quantify the antimicrobial effect. • The silver nanoparticles exhibited zone diameters ranging from 7.41 to 13.73 mm. • The selenium nanoparticles exhibited zone diameters ranging from 7.53 to 12.03 mm. • Different uppercase letters are used to indicate significant vertical differences between concentrations within the same nanoparticle. • Distinct lowercase letters denote notable horizontal disparities between the two nanoparticles at equal concentrations. To summarize, both categories of nanoparticles effectively suppressed the growth of Salmonella, with greater concentrations yielding more pronounced outcomes. However, silver exhibited greater potency at every level of concentration. The footnote clarifies that the LSD value is the minimum significant difference, meaning that any differences larger than 0.272 mm between groups or concentrations would be deemed statistically significant.

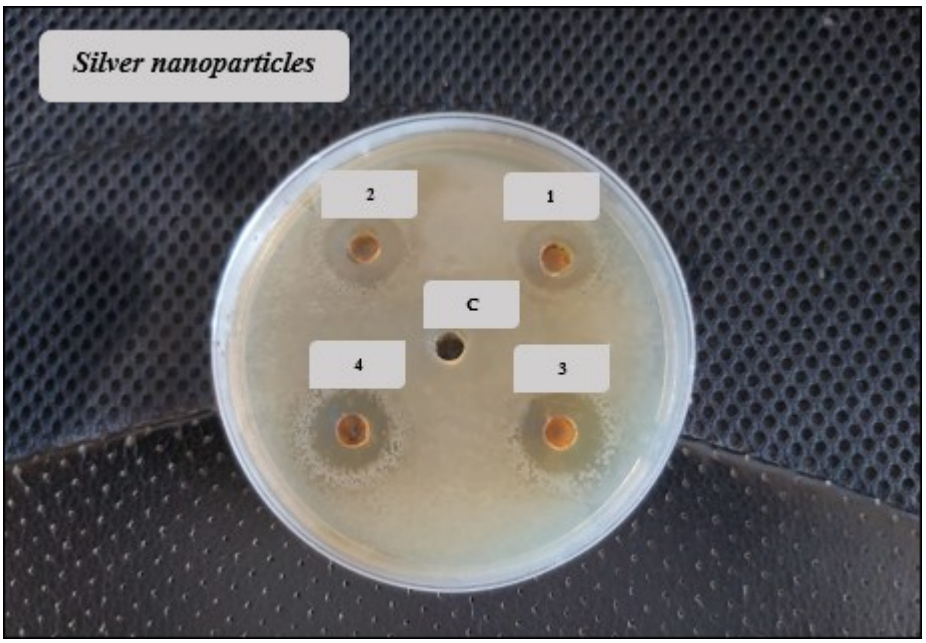


Figure 6. Efficacy of successive concentrations of silver nanoparticles against Salmonella in agar plates (1) Concentration 25 mg/ml (2) Concentration 50 mg/ml (3) Concentration 100 mg/ml (4) Concentration 200 mg/ml (C) Phosphate buffered saline solution PBS

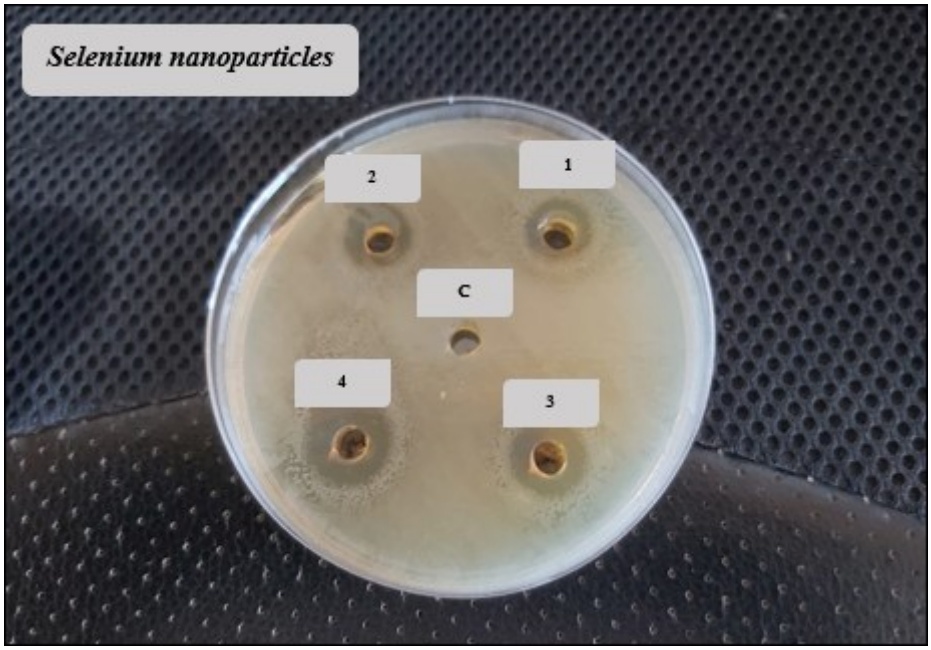


Figure 7. Efficacy of successive concentrations of selenium nanoparticles against Salmonella in agar plates (1) Concentration 25 mg/ml (2) Concentration 50 mg/ml (3) Concentration 100 mg/ml (4) Concentration 200 mg/ml (C) Phosphate buffered saline solution PBS

Discussion

The findings demonstrate a concentration-dependent antibacterial effect for both AgNPs and SeNPs. The inhibition zones increased from the lowest to the highest tested concentrations, indicating that a greater nanoparticle dose increased the capacity to suppress bacterial growth. AgNPs generally showed stronger antibacterial performance, as reflected by their lower MIC and MBC ranges and their larger inhibition zones at 50, 100, and 200 mg/mL. This pattern is consistent with previous evidence describing AgNPs as potent antimicrobial materials [2] and with studies showing that silver nanoparticles can inhibit bacterial growth through interactions involving silver ions, cellular membranes, and other cellular targets [5]. The relatively small mean diameter of the AgNPs (22.44±0.68 nm) compared with the SeNPs (41.34±1.28 nm) may also contribute to the observed difference because nanoparticle size influences surface area and biological interaction [3]. The UV-Visible, SEM, FT-IR, and XRD findings collectively confirm that the prepared materials exhibited distinct optical, morphological, chemical, and crystalline characteristics. SeNPs nevertheless demonstrated measurable antibacterial activity, supporting reports that selenium nanostructures can exhibit synergistic antibacterial properties when appropriately synthesized and stabilized [13]. The MIC and MBC results further strengthen the agar diffusion findings because they provide broth-based evidence of inhibitory and bactericidal concentrations [17]. Taken together, the results indicate that both nanoparticle types have antibacterial potential, while AgNPs were more potent under the conditions used in this study.

CONCLUSION

Fundamental Finding: Silver and selenium nanoparticles were successfully synthesized and characterized using UV-Visible spectroscopy, SEM, FT-IR, and XRD. AgNPs showed a mean particle size of 22.44±0.68 nm, whereas SeNPs averaged 41.34±1.28 nm. Both materials produced concentration-dependent antibacterial effects, but AgNPs demonstrated greater overall potency through lower MIC/MBC values and larger inhibition zones at most tested concentrations. **Implication:** These findings support the potential of chemically synthesized metallic nanoparticles as antibacterial materials and indicate that particle type and physicochemical characteristics are important determinants of activity. **Limitation:** Further studies should clarify the bacterial species-specific response and standardize nanoparticle concentration units. **Future Research:** Further studies should evaluate cytotoxicity and biocompatibility, and confirm efficacy using larger isolate sets and in vivo models before biomedical application.

REFERENCES

[1] J. A. Dahl, B. L. S. Maddux, and J. E. Hutchison, "Toward greener nanosynthesis," Chemical Reviews, vol. 107, no. 6, pp. 2228-2269, 2007.

[2] M. Rai, A. Yadav, and A. Gade, "Silver nanoparticles as a new generation of antimicrobials," Biotechnology Advances, vol. 27, no. 1, pp. 76-83, 2009.

[3] V. K. Sharma, R. A. Yngard, and Y. Lin, "Silver nanoparticles: Green synthesis and their antimicrobial activities," Advances in Colloid and Interface Science, vol. 145, nos. 1-2, pp. 83-96, 2009.

[4] G. Bugla-Ploskonska et al., "Bactericidal properties of silica particles with silver islands located on the surface," International Journal of Antimicrobial Agents, vol. 29, no. 6, pp. 746-748, 2007.

[5] O. Choi, K. K. Deng, N. J. Kim, L. Ross Jr., Y. Z. Surampalli, and R. Hu, "The inhibitory effects of silver nanoparticles, silver ions, and silver chloride colloids on microbial growth," Water Research, vol. 42, nos. 12-13, pp. 3066-3074, 2008.

[6] T. T. N. Dung et al., "Synthesis of nanosilver particles by reverse micelle method and study of their bactericidal properties," Journal of Physics: Conference Series, vol. 187, Art. no. 012054, 2009.

[7] B. S. Atiyeh, M. Costagliola, S. N. Hayek, and S. A. Dibo, "Effect of silver on burn wound infection control and healing: Review of the literature," Burns, vol. 33, no. 2, pp. 139-148, 2007.

[8] R. E. Burrell, R. Demling, S. Pancani, A. Papp, O. Strand, and V. Voinchet, "The role of Acticoat with nanocrystalline silver in the management of burns," Burns, vol. 30, Suppl. 1, pp. S1-S9, 2004.

[9] W. Yan et al., "A novel, practical and green synthesis of Ag nanoparticles catalyst and its application in three-component coupling of aldehyde, alkyne, and amine," Journal of Molecular Catalysis A: Chemical, vol. 225, pp. 81-85, 2006.

[10] H. Liu, D. Ma, R. A. Blackley, W. Zhou, and X. Bao, "Highly active mesostructured silica hosted silver catalysts for CO oxidation using the one-pot synthesis approach," Chemical Communications, pp. 2677-2679, 2008.

[11] S. P. Ramnani et al., "Advantage of radiolysis over impregnation method for the synthesis of SiO2 supported nano-Ag catalyst for direct decomposition of N2O," Catalysis Communications, vol. 9, pp. 756-761, 2008.

[12] H. J. Kim, S. H. Park, and H. J. Park, "Synthesis of a new electrically conducting nanosized Ag-polyaniline-silica complex using gamma-radiolysis and its biosensing application," Radiation Physics and Chemistry, vol. 79, pp. 894-899, 2010.
[13] M. Vahdati and T. Tohidi Moghadam, "Synthesis and characterization of selenium nanoparticles-lysozyme nanohybrid system with synergistic antibacterial properties," Scientific Reports, vol. 10, Art. no. 510, 2020.
[14] J. Fang, C. Zhong, and R. Mu, "The study of deposited silver particulate films by simple method for efficient SERS," Chemical Physics Letters, vol. 401, pp. 271-275, 2005.
[15] J. Kiefer, J. Grabow, H.-D. Kurland, and F. A. Müller, "Characterization of nanoparticles by solvent infrared spectroscopy," Analytical Chemistry, vol. 87, no. 24, pp. 12313-12317, 2015.
[16] N. S. Abdulrazzaq and M. A. Al-Azzawi, "Effect of zirconium oxide-titanium dioxide nanoparticles on mechanical and physical properties of soft denture lining materials," Journal of Nanostructures, vol. 12, pp. 34-44, 2022, doi: 10.22052/JNS.2022.01.005.
[17] P. Parvekar, J. Palaskar, S. Metgud, R. Maria, and S. Dutta, "The minimum inhibitory concentration (MIC) and minimum bactericidal concentration (MBC) of silver nanoparticles against Staphylococcus aureus," Biomaterials Investigations in Dentistry, vol. 7, no. 1, pp. 105-109, 2020, doi: 10.1080/26415275.2020.1796674.
[18] Q. E. Al-Bayati, "Detection of virulence factors of Pseudomonas aeruginosa bacteria isolated from wound infections and study of the effect of silver nanoparticles on them," M.S. thesis, College of Science, Tikrit University, Tikrit, Iraq, 2016.

*** Khawla S. Mohammed (Corresponding Author)**
Tikrit University, Iraq
Email: Khawla.mohammed122@tu.edu.iq